REFRACTIVE INDEX MATCHED PIV MEASUREMENTS OF FLOW AROUND INTERACTING BARCHAN DUNES

Nathaniel Bristow

Department of Aerospace and Mechanical Engineering
University of Notre Dame
Notre Dame, Indiana, USA
nbristow@nd.edu

Gianluca Blois

Department of Aerospace and Mechanical Engineering
University of Notre Dame
Notre Dame, Indiana, USA
gblois@nd.edu

James Best

Departments of Geology, Geography and GIS, Mechanical Science and Engineering and
Ven Te Chow Hydrosystems Laboratory
University of Illinois
Champaign, Illinois, USA
jimbest@illinois.edu

Kenneth Christensen

Department of Aerospace and Mechanical Engineering
University of Notre Dame
Notre Dame, Indiana, USA
kchrist7@nd.edu

ABSTRACT

Barchan dunes are crescent shaped bedforms found in both aeolian and subaqueous environments, including deserts, river beds, continental shelves, and even the craters of Mars. The evolution of and dynamics associated with these mobile bedforms involve a strong degree of coupling between sediment transport, morphological change, and flow, the last of which represents the weakest link in our current understanding of barchan morphodynamics. Their three-dimensional geometry presents experimental challenges for measuring the full flow field, particularly around the horns and in the leeside of the dunes. In this study we present measurements of the turbulent flow surrounding fixed barchan dune models in various configurations using particle image velocimetry in a refractive index matching flume environment. The refractive index matching technique opens the door to making measurements in wall-parallel planes surrounding the models, as well as wall-normal plane measurements in the leeside region between the horns. While fixed bed experiments are unable to directly measure sediment transport, they allow us to focus solely on the flow physics and full resolution of the turbulent flow field in ways that are otherwise not possible in mobile bed experiments.

INTRODUCTION

Barchan dunes are three-dimensional bedforms which are formed in environments characterized by unidirectional flow and a limited supply of sediment. Their planform crescentic morphology consists of two "horns" pointing downstream, with a gentle upstream "stoss" slope and a steeper leeside. As mobile bedforms, barchans migrate downstream over time, and are typically found within the context of a larger field of dunes. Important for a number of geophysical and engineering applications (Lancaster, 2009), observations have historically associated barchans with aeolian desert environments, though new methods in measuring river bed topography (i.e. multibeam echo sounding) has revealed their existence in subaqueous environments, and recent high-resolution satellite imagery has identified barchan fields on the surface of the craters of Mars as well.

Studies of the interaction between turbulent flows and barchan morphology are limited, with only a handful of recent laboratory experiments and numerical simulations (Palmer et al., 2012; Charru and Franklin 2012; Omidyeganeh et al 2013, Wang et al., 2016; Khosronejad and Sotiropoulos, 2017), as modelling efforts have largely ignored the role of unsteady turbulence and the existence of coherent structures in the flow. Instead, flow over the bedform is considered as having a more simple "inner" and "outer" layer structure, as in the Jackson and Hunt (1975) model for flow over a gentle hill. The assumption is generally made that turbulent fluctuations are not important, and a mean bed shear stress model is sufficient to predict sediment transport, where $q_s \sim u_\tau^3$, with q_s as sediment flux and u_τ as the mean bed shear stress (Bagnold 1941; Owen 1964; Weng et al., 1991).

Problems arise when applying this to situations where flow separation is important, wherein the "gently sloping hill" model does not apply. Models for barchans (Kroy et al., 2002; Duran et al., 2010) compensate for this by adding a "separation bubble" in the dune leeside, where there is assumed zero sediment flux, and the flow outside the separation bubble mimics that over the leeside of a gently sloping hill. But this is a poor substitute for the strong shear layer and coherent vortical structures which are typically generated in the wakes of obstacles with flow separation, and therefore the influence of turbulent fluctuations is underestimated. Moreover, the ability of the wake flow from an upstream barchan to act at a distance to influence erosion of a downstream barchan is not accurately represented.

This can be demonstrated by comparing modelling results with a flume experiment (Hersen and Douady, 2005) of a situation where a smaller upstream barchan approaches and collides with a downstream barchan (barchan size is inversely

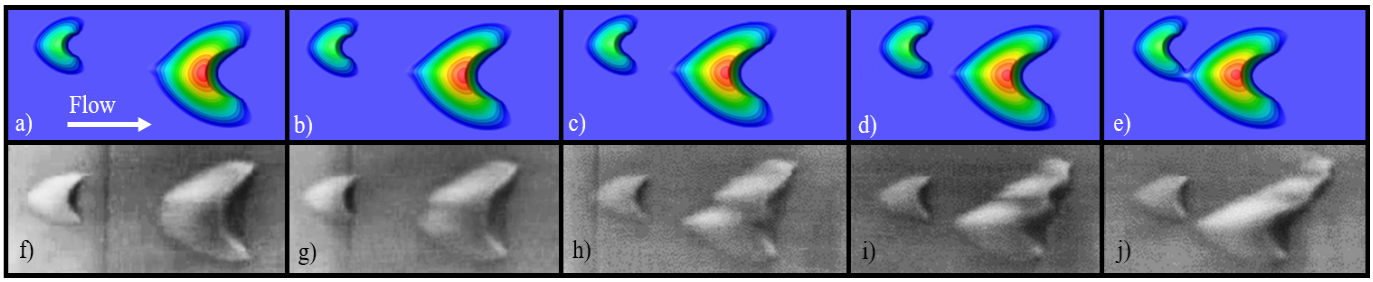

Figure 1. Comparison of (a-e) morphodynamic model and (f-j) mobile-bed flume experiments (Hersen and Douady, 2005), highlighting model deficiencies for a barchan collision. Code courtesy Dr. H. J. Herrmann (Parteli et al., 2014) (modified by us for this scenario).

related to migration rate (Andreiotti et al., 2002)), as is shown in Figure 1. Here the numerical simulation is performed using a model based on the work of Parteli et al. (2014). The comparison highlights the contrasting dynamics, where in the flume experiment, the upstream barchan dune (UBD) acts at a distance to cause erosion and deformation of the downstream barchan dune (DBD) prior to physical contact between the two bedforms. The simulation fails to capture this behavior, as is most apparent in Figure 1e, where both barchans in the simulation remain undeformed. Naturally, this begs the question as to the structure of the flow in this interdune region that is driving this process.

Experimental measurements of the flow are challenged by the complex three-dimensionality of the barchan morphology, which inhibits full optical access to the flow field. This is particularly problematic in cases with multiple barchans interacting with each other. To date, laboratory experiments have considered only inline "collisions" between barchans, where there is no lateral offset between them (Palmer et al., 2012). This retains symmetry in the flow and simplifies making measurements, but is not typical of the way barchans interact in nature, where it is more common for there to be a lateral offset.

In this paper, we present measurements of the flow field associated with a laterally offset collision between a smaller, upstream barchan dune (UBD) and a larger, downstream barchan dune (DBD). In these experiments, fixed-bed models of the barchans are used to study three separate stages of in the collision process, wherein the morphology of the DBD is altered in each stage to mimic the behavior observed in the mobile-bed experiments of Hersen and Douady (2005). To serve as a baseline case for comparison, measurements were also made around an isolated barchan model.

METHODS

Experiments were conducted in the Small-scale Refractive Index Matching (S-RIM) flow facility at the University of Notre Dame. The RIM approach allows full optical access to the entire flow region surrounding three-dimensional models, as they are rendered fully transparent such that the aberrations, reflections, and refraction of light passing through the models are minimized. To achieve this, an aqueous solution of Sodium Iodide (NaI) (63% by weight) is used as the working fluid as its refractive index (RI) is very close to that of clear acrylic models. The flow is tripped at the inlet of the test section, which has 112 mm wide square cross section, such that a turbulent boundary layer develops with a thickness of 45.6 mm at the measurement location, resulting in a Reynolds number $Re_\delta \approx 41{,}500$ and $Re_\tau \approx 1633$.

The barchan models used in the experiments possessed morphologies based on the 3D topography generated by Hersen (2004) which fits in the range of typical dimensional aspect ratios found in nature. The isolated case utilized this baseline morphology, with which an upstream barchan was then generated having the same shape but half the length, width and height, and 1/8th the original volume. The first collision stage, hereafter referred to as collision A, featured no deformations to the DBD. In the following two collision stages, hereafter referred to as collisions B and C, the horn of the DBD that is downstream of the UBD was increasingly elongated. All four configurations, including the isolated case and three collision cases, are shown in Figure 2.

Particle image velocimetry (PIV) was used to make measurements of the flow in both wall-normal (*x*-*y*) and wall-parallel (*x*-*z*) at varying spanwise offsets and elevation heights respectively. A single 29 MP camera with a 0.5 Hz sampling rate was used to capture 5000 image pairs at each measurement location. The PIV processing was performed using initial and final spot sizes of 64x64 and 32x32 pixels respectively, after

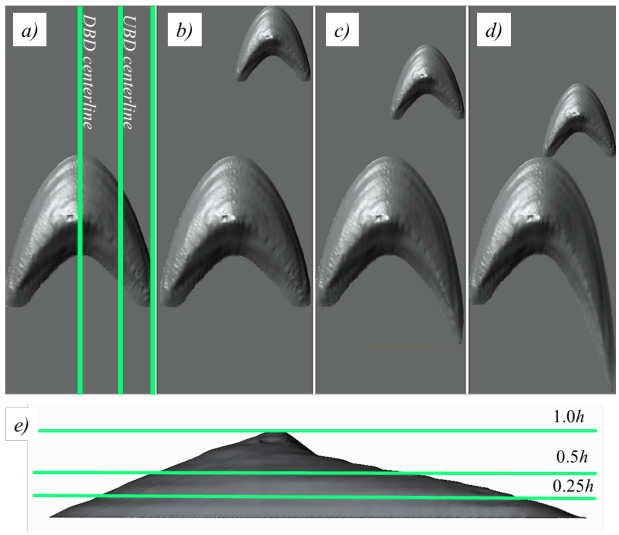

Figure 2: Isolated and collision barchan configurations, with measurement planes indicated by green lines. Presented in this paper are measurements in DBD centerline, UBD centerline, and 0.25*h* planes.

which vector post-processing removed spurious vectors with a normalized median filter, achieving a final valid vector yield of at least 95% for each data set within the wake region where turbulence was most intense.

RESULTS

The isolated barchan case served as the baseline with which to compare each of the collision stages. Collision A demonstrates the influence of adding a UBD, and collisions B and C explore the effect of changing interdune separation while the DBD morphology is changed as well.

Mean streamwise velocity contours with streamlines overlaid show the mean structure of the flow and the first order effects of topographic forcing. A three-dimensional recirculation "bubble" exists in the lee of the isolated dune (Figure 3), extending roughly 4.8*h* downstream from the crest, ending where the flow reattaches in the centerline plane. This region of the flow is characterised by low momentum, reverse flow moving back upstream at up to $0.3U_\infty$, where U_∞ is the mean free stream velocity. As is shown by comparison of the centerline plane (Figure 3a) and the spanwise offset set plane (which is aligned in the collision cases with the UBD centerline) (Figure 3b), the reattachment length decreases with distance away from the centerline. The wall-parallel planes demonstrate the significant amount of spanwise motion within the wake, and yet also strong asymmetry about the centerline.

With the introduction of an UBD in collision A, a moderate sheltering effect begins to be seen downstream of the UBD centerline (Figure 4a-c). Comparison with the isolated case at this same wall-normal plane shows that the recirculation cell in the lee of the DBD horn contracts slightly. In the two subsequent stages, collisions B and C, streamlines show that the flow separation over the DBD horn decreases further until there no longer appears to be a recirculation cell. Meanwhile, the recirculation bubble of the UBD moves into very close proximity with the DBD in collision C, until it's centerline reattachment point lies where DBD topography begins near the horn.

The wall-parallel planes (at y/h = 0.25, Figure 4d-f) highlight an important aspect of the collision process, whereby a flow channelling effect and "wake veering" (Wang et al 2016) is observed in the interdune space, and significant asymmetry develops in the wake of the DBD. While this is relatively minor in collision A, by collision C the wake region of the UBD clearly no longer resembles that of an isolated barchan, where its symmetry is broken and flow is being channelled laterally in its wake around the DBD.

Vertical profiles of Reynolds stresses in the interdune space highlight the differences in spatial distribution of turbulent stresses across the isolated and collision cases. Figure 5 shows vertical profiles of $\langle uv \rangle$, $\langle u^2 \rangle$, and $\langle v^2 \rangle$ (where brackets indicate ensemble averaging) from three *x*-positions along the UBD centerline plane. The first x-position (Figure 5a,d,g), located in the interdune space, upstream of where DBD topography begins, highlights the biggest differences with the clearest trends. The isolated case shows nearly constant levels of Reynolds shear stress, with small change with elevation above the bed. In contrast, each of the collision cases display a clear elevation height of where $\langle uv \rangle$ reaches a maximum. For collision A, this is found at roughly y^+/h = 0.6 where the value of $\langle uv \rangle$ is nearly

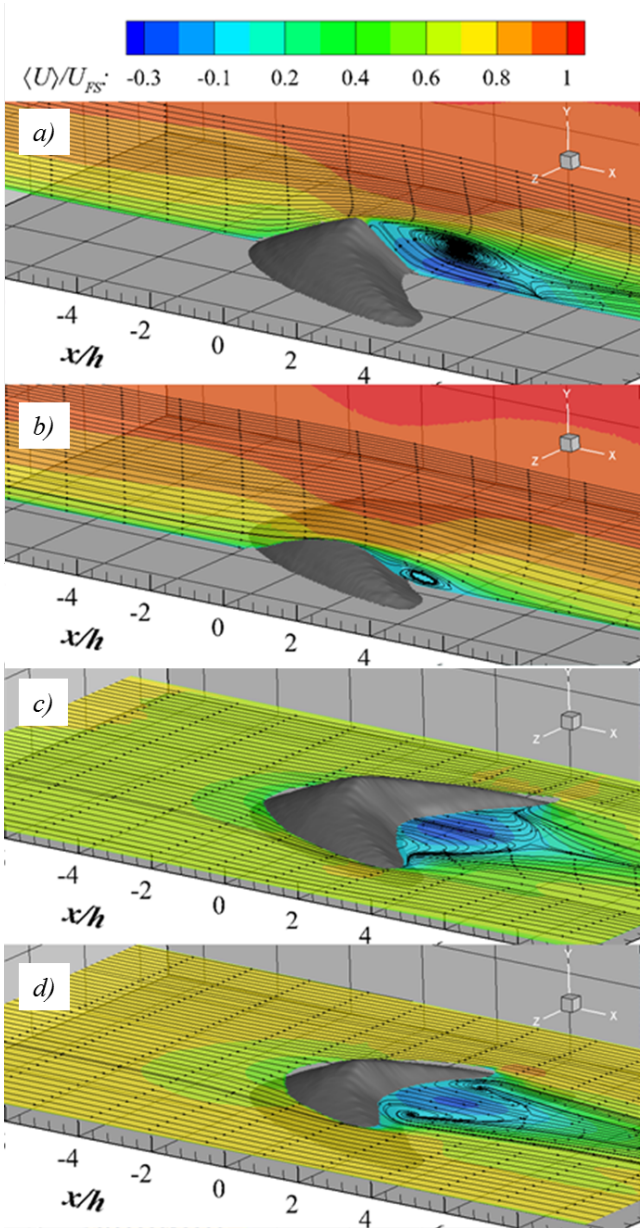

Figure 3: Mean streamwise velocity contours for isolated barchan, overlaid with mean streamlines, for 4 measurement planes: (a) centerline wall-normal symmetry plane, (b) wall-normal plane offset from centerline (aligned with centerline plane of UBD in collision configurations), (c) 0.25h elevation wall-parallel plane, and (d) 0.5h elevation wall-parallel plane.

four times higher than that of the isolated case. In collisions B and C, this location of maximum shear stress moves closer to the bed, and the value increases in magnitude. Both of the Reynolds normal stresses show similar trends of higher stress values nearer to the bed as the UBD approaches. The $\langle u^2 \rangle$ profile for the isolated case at this first *x*-position shows that streamwise Reynolds normal stresses increase towards the bed, whereas all three collision cases have distinct peak values raised from the bed. For all three of the Reynolds stress components, the stresses

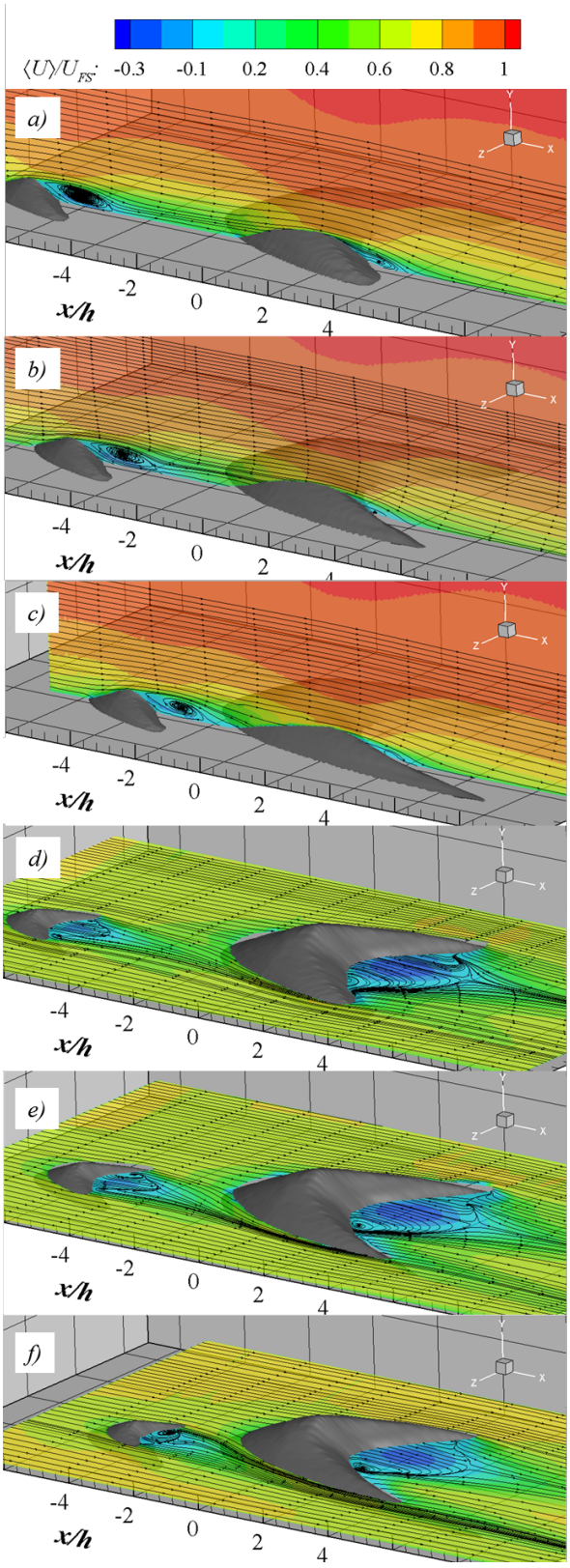

Figure 4: Mean streamwise velocity contours with streamlines overload for (a-c) the wall-normal UBD centerline plane and (d-f) the wall-parallel 0.25*h* elevation plane, for all three collision cases.

are more evenly distributed vertically for collisions A and B, as compared to collision C. In other words, the vertical profiles for collision C have narrower peaks.

At the next *x*-position, overlying the DBD topography, a similar trend can again be observed for all three Reynolds stress components plotted, although the differences between the isolated case and each of the collision cases is lower than was observed at the previous *x*-position. In particular, collisions A and B do not show significantly different peak locations, although collision B has consistently higher magnitudes. Collision C again has higher magnitudes nearer to the bed. In the final *x*-position plotted, near the crest of the DBD horn, the differences between the isolated and collision cases have again decreased, as well as the magnitudes in general. This indicates a dissipation of the Reynolds stresses as the stoss slope of the DBD is climbed, coincident with a favourable pressure gradient accelerating the flow up the incline.

It is important to note that, as was shown previously in the contour maps of mean velocity, the flow is highly three-dimensional, especially in the interdune space as the UBD approaches, and therefore while these measurements in the wall-normal plane provide some insight into trends in turbulent stresses near the bed, they do not form a complete picture. Wall-parallel measurements are important in this regard.

Plotted in Figure 6 are contour maps of the wall-parallel component of the Reynolds shear stress. In this plane, it is clear to see how the spatial distribution of shear stresses in the wake of the DBD is significantly modified as the UBD approaches the DBD. While in collision A this UBD wake is symmetric and similar to that the isolated barchan, in collision C this symmetry is broken, and elevated levels of shear stress are extended along the outside of the DBD horn. Thus the wake is shifted laterally, indicating that the location of maximum Reynolds stresses would not necessarily be measured in the UBD centerline plane, and therefore the differences between the collision cases that were noted in Figure 5 could be even more pronounced than was shown.

CONCLUSIONS

This study provides accurate 2D flow measurements of the turbulent flow surrounding fixed, interacting barchan dune models. Using planar PIV in conjunction with a refractive index matching technique, the mean flow structure around barchan dunes in an offset collision situation was measured and is presented here.

The turbulent wake of the barchan dune is a complex 3D flow field that does not lend itself toward being modelled with approaches that have been used in the past for aeolian morphodynamics. In the collision case presented here, which is one of the most common types of barchan interactions, the heterogeneity in the flow and the influence of offset bedforms to significantly modify the flow field is clear.

Further work remains to fully extract the dominant flow structures and mechanisms correlating to sediment transport and morphological change associated with these types of interactions. Future experiments to aid in this endeavour include time-resolved and 3D PIV measurements which will help to characterize and resolve important structures in the flow.

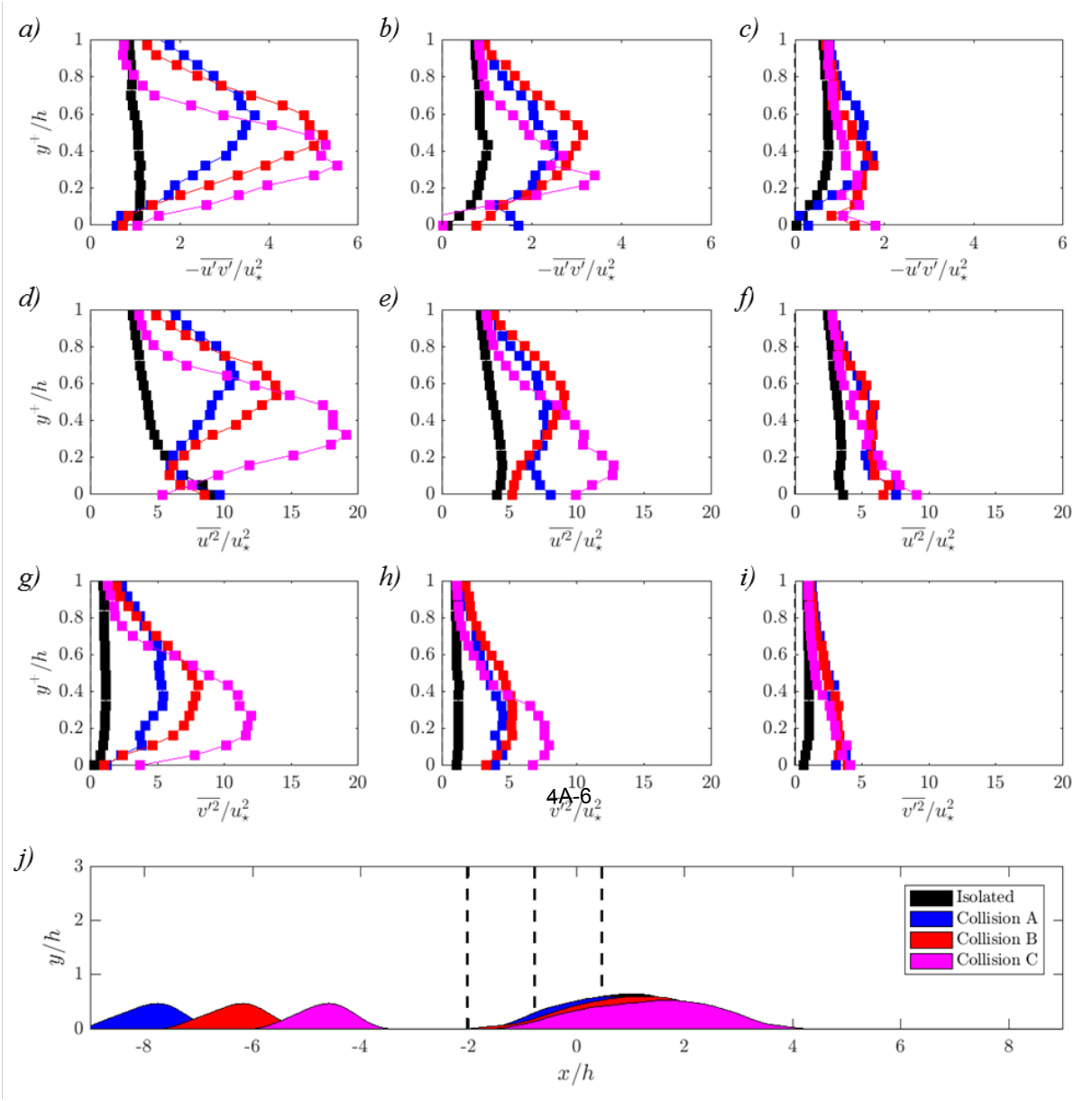

Figure 5: Vertical profiles of (a-c) Reynolds shear stress, (d-f) streamwise Reynolds normal stress, and (g-i) vertical Reynolds normal stress, for all four cases, plotted as a function of relative elevation height above the local topography (y^+/h) at four x-positions (-2h, -0.75h, 0.5h) corresponding to dashed lines in (j), where color contours indicate topography of each barchan configuration along the UBD centerline measurement plane. All stresses are normalized by the upstream skin friction, u_τ.

ACKNOWLEDGEMENTS

This work was supported by the National Science Foundation through grant CBET-1603211.

REFERENCES

Andreotti, B., Claudin, P., and Douady, S., 2002. "Selection of dune shapes and velocities Part 1: Dynamics of sand, wind and barchans", *The European Physical Journal B,* Vol. 28, pp. 321-339.

Bagnold, R. A., 1941. "The physics of wind blown sand and dust", *Methuen & co. ltd.,* London.

Charru, F. and Franklin, E. M., 2012. "Subaqueous barchan dunes in turbulent shear flow. Part 2. Fluid flow", *Journal of Fluid Mechanics*, Vol. 694, pp.131–154.

Duran, O., Parteli, E. J. R., and Herrmann, H. J., 2010. "A continuous model for sand dunes: Review, new developments and application to barchan dunes and barchan dune fields", *Earth Surface Processes and Landforms,* Vol. 35, pp. 1591-1600.

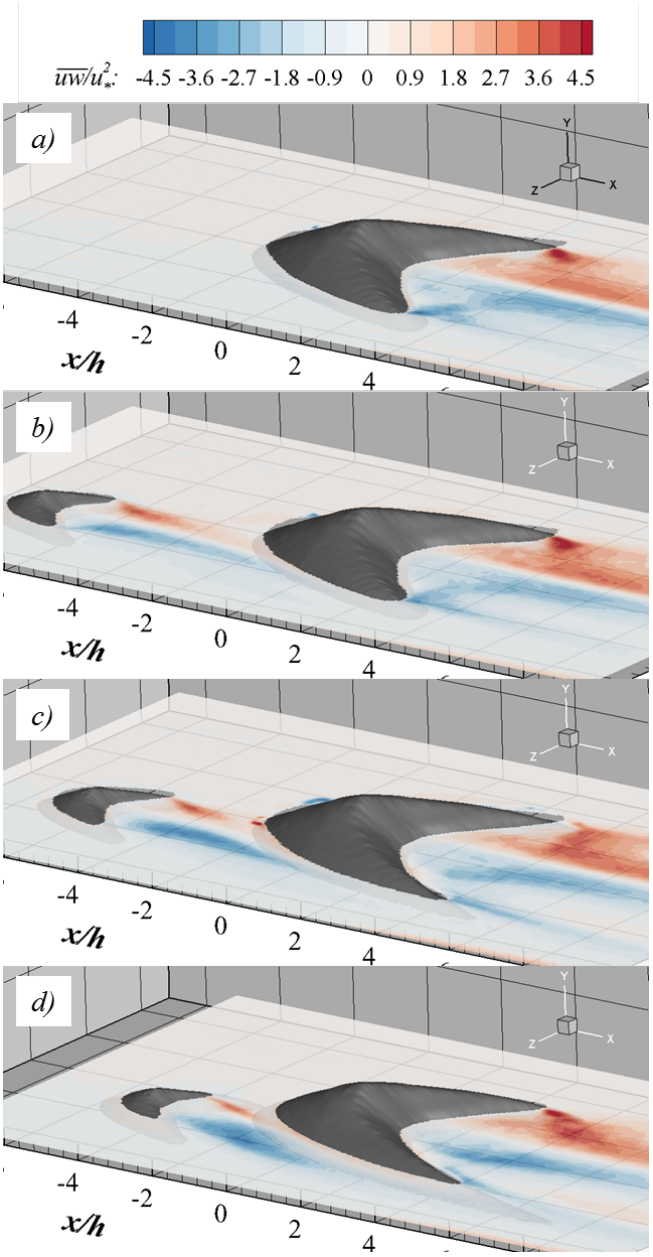

Figure 6: Contour maps of Reynolds shear stress <uw> in the wall-parallel 0.25*h* elevation plane, for (a) the isolated case, and (b-d) the three collision cases.

Endo, N., Taniguchi, K., and Katsuki, A., 2004. "Observation of the whole process of interaction between barchans by flume experiments", *Geophysical Research Letters*, Vol. 31.

Hersen, P., 2004. "On the crescentic shape of barchan dunes", *The European Physical Journal B*, Vol. 37, pp. 507-514.

Hersen, P. and Douady, S., 2005. "Collision of barchan dunes as a mechanism of size regulation", *Geophysical Research Letters*, Vol. 32.

Jackson, P. S. and Hunt, J. C. R., 1975. "Turbulent wind flow over a low hill", *Quarterly Journal of the Royal Meteorological Society,* Vol. 101, pp. 929-955.

Khosronejad, A. and Sotiropoulos, F., 2017. "On the genesis and evolution of barchan dunes: morphodynamics", *Journal of Fluid Mechanics,* Vol. 815, pp. 117-148.

Kroy, K., Sauermann, G., and Herrmann, H. J., 2002. "Minimal model for sand dunes", *Physical Review Letters,* Vol. 88(5).

Lancaster, N., 2009. "Geomorphology of desert environments", In *Geomorphology of Desert Environments*. pp. 557–596.

Omidyeganeh, M., Piomelli, U., Christensen, K. T., and Best, J. L., 2013. "Large eddy simulation of interacting barchan dunes in a steady, unidirectional flow", *Journal of Geophysical Research: Earth Surface,* Vol. 118, pp. 2089-2104.

Owen, P.R., 1964. "Saltation of uniform grains in air", *Journal of Fluid Mechanics*, Vol. 20, pp. 225-242.

Palmer, J. A., Mejia-Alvarez, R., Best, J. L., and Christensen, K. T., 2012. "Particle-image velocimetry measurements of flow over interacting barchan dunes", *Experiments in Fluids*, Vol. 52(3), pp. 809–829.

Parteli, E. J. R., Duran, O., Bourke, M. C., Tsoar, H., Pöschel, T., and Herrmann, H. J., 2014. "Origins of barchan dune asymmetry : Insights from numerical simulations", *Aeolian Research*, Vol. 12, pp. 121–133.

Wang, C., Tang, Z., Bristow, N., Blois, G., Christensen, K. T., and Anderson, W., 2016. "Numerical and experimental study of flow over stages of an offset merger dune interaction", *Computers and Fluids*, pp. 1-12.

Weng, W. S., Hunt, J. C. R., Carruthers, D. J., Warren, A., Wiggs, G. F. S., Livingstone, I., Castro, I., 1991. "Air flow and sand transport over sand-dunes," *Acta Mechanica,* 2, pp. 1-22.